Temperature crossover of decoherence rates in chaotic and regular bath dynamics

A. S. Sanz,[1] Y. Elran,[2] and P. Brumer[3]

[1]*Instituto de Física Fundamental (IFF–CSIC), Serrano 123, 28006 Madrid, Spain*
[2]*The Weizmann Institute of Science, Rehovot, Israel*
[3]*Chemical Physics Theory Group, Department of Chemistry,
and Center for Quantum Information and Quantum Control,
University of Toronto, Toronto, Ontario, Canada M5S 3H6.*

The effect of chaotic bath dynamics on the decoherence of a quantum system is examined for the vibrational degrees of freedom of a diatomic molecule in a realistic, constant temperature collisional bath. As an example, the specific case of I_2 in liquid xenon is examined as a function of temperature, and the results compared with an integrable xenon bath. A crossover in behavior is found: the integrable bath induces more decoherence at low bath temperatures than does the chaotic bath, whereas the opposite is the case at the higher bath temperatures. These results, verifying a conjecture due to Wilkie, shed light on the differing views of the effect of chaotic dynamics on system decoherence.

I. INTRODUCTION

Decoherence, and the control of decoherence, is a central problem in modern quantum physics. In particular, "quantum technologies", such as quantum cryptography, quantum computing [1] and quantum control [2] rely upon the maintenance of quantum effects over significant periods of time. As such, decoherence serves as a primary obstacle to progress in the experimental implementation of a number of these quantum based scenarios. Of particular interest is the nature and rates of decoherence in systems in the condensed phase.

In this regard, it has been long argued [3–14] that traditional uncoupled oscillator or standard spin bath models (e.g., the spin-boson [15, 16], boson-boson [17–19], spin-spin [20] models) are inadequate to describe dynamics in condensed phases since they lack intra-environmental coupling. Such intra-environmental coupling can display different types of behavior, including chaotic dynamics, and therefore its effect on decoherence can be significantly different from traditional models.

For example, in such uncoupled bath cases, when the system perturbs the bath, it cannot relax internally; energy must flow through the subsystem in order for the bath to return to equilibrium. This causes the system energy to increase initially even when relaxation is expected [21]. Second, the system becomes strongly entangled with the bath as a result of this energy flow and hence the system decoheres more strongly than it should. Finally, the equilibrium state that the bath reaches may not be the expected canonical state [22].

Applications of uncoupled oscillators to model condensed phase environments may be especially problematic. For example, anharmonic corrections are known to be important in the study of phonons in Si [23] and are essential for the explanation of heat transport. Both the vibrational dynamics of Si [24] and its electronic structure [25] are believed to be chaotic. Dynamics of a colloidal particle in water have also been shown to be chaotic [26].

The effect of the structured environment on some issues in solid state has been examined. For example, it has recently been shown, for the central spin model [27–33], that the role of structured environments on solid-state (ferromagnetic phase) implementations is important. In particular, the dynamical regime of the bath has been observed [28] to determine the efficiency of the decoherence process. For example, in a perturbative regime, decoherence is stronger in the integrable limit; on the other hand, in the strong coupling regime the chaotic limit is more efficient. Also, the two-spin system decoherence has been found to exhibit different behavior depending on the characteristics of the coupling with the environment, as well as on the internal dynamics and initial state of the environment.

Clearly, studies on more realistic models than the uncoupled oscillator or spin models are needed for condensed phase environments. Efforts to generalize the oscillator bath model in such cases are very preliminary. When intra-bath coupling is added to the boson or spin bath, general analytic solutions are unavailable and exact solutions can only be obtained computationally for very small baths. In the case of oscillator bath models, the bath cannot consist of more than three or four oscillators. For spin baths results have been reported for approximately 20 spins.

The most common question addressed in such studies is whether intra-bath coupling increases or decreases the decoherence of the embedded subsystem. Surprisingly, this apparently simple question has generated considerable controversy. It was first conjectured by Zurek that decoherence should be greater for chaotic baths [3]. This was quantitatively verified in a study wherein a single harmonic oscillator subsystem interacts with a bath consisting of a single chaotic oscillator [5]. Unfortunately, the relevance of this result to the usual paradigm of a small system interacting with a large environment is un-

clear. Furthermore, Alicki has argued [7], by contrast, that the decoherence rate in the limit of pure decoherence (i.e. in the absence of dissipation) will be greater for an integrable bath than for a chaotic bath. This is because the energetically available bath states in the integrable case can be highly degenerate, whereas only one state is available in the chaotic bath at a given energy due to level repulsion. Thus if a chaotic system-bath state is microcanonical, the wavefunction of the system plus bath will be a simple product state, since there is only one energetically available bath state with which the system can couple. Accordingly, there should be greater decoherence in the integrable case. This viewpoint can also be supported with semiclassical arguments [6]. It can be shown that the square of the off-diagonal matrix elements of the system-bath coupling operator scale as $\hbar^{N-1}$ for a chaotic bath [34]. The off-diagonal coupling matrix elements thus vanish in the thermodynamic limit. At low temperatures the diagonal matrix elements change slowly with energy [6] and so the subsystem dynamics is shifted but not strongly decohered. By contrast, selection rules for integrable systems guarantee large off-diagonal matrix elements which cause strong decoherence. These conclusions were verified numerically for a low temperature spin-bath [6].

Thus, there are two well-defined and apparently contradictory positions on the issue of whether a chaotic bath may increase or decrease decoherence. Numerous low temperature spin-bath studies [4, 6, 8–12, 14] support Alicki's [7] predictions that decoherence should be greater for integrable baths. However, there are spin-bath studies that draw the opposite conclusion [13] and hence support Zurek's conjecture that chaotic baths cause greater decoherence.

Based on these results Wilkie has speculated [35] that some sort of transition occurs with increasing temperature; a chaotic bath could cause less decoherence at low temperature and greater decoherence at high temperature. This conjecture would be consistent with the spin-bath results [4, 6, 8–14] and would not be in direct conflict with the oscillator calculation [5]. However, the existence of such a transition is difficult to verify in exact spin-bath or oscillator-bath calculations. High temperature calculations for a bath of ten spins [6] did not show such a transition and calculations for larger spin-baths could not be carried out at high temperature.

An alternative approach would be to explore the possibility of such a transition using an approximation scheme. This approach is the focus of this paper. Recently it has been shown that quantum decoherence can be accurately computed using classical dynamics simulations based on the quantum Wigner function [36, 37]. In this Wigner approach, regions of phase space where the Wigner function of the initial state takes negative values are Monte Carlo sampled using the absolute value and the resulting classical trajectories carry a negative sign as a weighting factor. The resulting approximation can be very accurate, and in this paper we employ this approach to ex-

amine the decoherence of a superposition of vibrational states of I_2 in liquid Xe baths comprising 512 atoms.

Our key observations are: (a) we observe less decoherence of vibrational superposition states of I_2 at low temperatures for liquid Xe than for its ideal gas counterpart obtained via simulations without Xe-Xe interactions, but (b) as the temperature is increased, a transition is observed and liquid Xe becomes the stronger source of decoherence. Thus, we show the existence of the two regimes in a physically realistic model. Note, as an immediate application, that the decoherence of a vibrational superposition state is a significant impediment to coherent control via pump-dump scenarios [2]. Hence, understanding conditions responsible for decoherence in such systems is important. Indeed, this was the original motivation for examining this particular system.

This paper is organized as follows. The model considered, as well as the details of the numerical simulations, are discussed in Sec. II. Section III reports the numerical results of the simulations for two different initial states at three temperatures and qualitative explanations for the observed behavior are proposed. Finally, Sec. IV contains a summary of conclusions.

II. MODEL

A. Hamiltonian

Consider the decoherence rates for different superpositions of vibrational states of I_2 coupled to a bath of Xe atoms. The subsystem of interest is the vibrational degree of freedom of the diatomic, and the environment comprises the translational degrees of freedom of the I_2 and of the Xe atoms. The Hamiltonian describing the full system [38] can be written as a standard system-plus-environment Hamiltonian, as follows:

$$H = H_s + H_e + H_{se}, \qquad (1)$$

where

$$H_s = \frac{p^2}{2\mu_{I_2}} + V(q), \qquad (2a)$$

$$H_e = \frac{p_{I_2}^2}{2m_{I_2}} + \sum_i \frac{p_i^2}{2m_{Xe}} + \sum_{i<j} \phi_{Xe-Xe}(r_{ij}), \quad (2b)$$

$$H_{se} = \sum_i \phi_{I_2-Xe}(r_{0i}, q). \qquad (2c)$$

Here, Eqs. (2a) and (2b) describe the independent evolution of the I_2 vibrational degree of freedom (q) and the bath dynamics, respectively, while Eq. (2c) accounts for their interaction. The isolated I_2 is described by a Morse oscillator,

$$V = D \left[1 - e^{-\beta(q-q_0)} \right]^2, \qquad (3)$$

with $D = 1.2547 \times 10^4$ cm^{-1}, $\beta = 1.8576$ Å^{-1}, $q_0 = 0$, and $\mu_{I_2} = m_{I_2}/4$, with m_{I_2} being the I_2 molecule mass and μ_{I_2} being its reduced mass. The degrees of freedom of the environment include the translational degree of freedom of the I_2 (its center of mass, with mass m_{I_2}), as well as the collection of N Xe atoms. The interaction between Xe pairs is described by the Xe-Xe interaction potential $\phi_{Xe-Xe}(r_{ij})$, where r_{ij} is the distance between the ith and jth Xe atoms. This interaction is modeled by a realistic pairwise Lennard-Jones potential:

$$\phi_{Xe-Xe}(r_{ij}) = 4\epsilon_{Xe-Xe}\left[\left(\frac{\sigma_{Xe-Xe}}{r_{ij}}\right)^{12} - \left(\frac{\sigma_{Xe-Xe}}{r_{ij}}\right)^6\right],$$
(4)

where $\epsilon_{Xe-Xe} = 154.00$ cm^{-1} is the well-depth of the potential and $\sigma_{Xe-Xe} = 3.930$ Å is related to the position of the minimum of the well $[V(r_{min}) = -\epsilon_{Xe-Xe}]$, $r_{min} = 2^{1/6}\sigma_{Xe-Xe}$. Here, ϵ_{Xe-Xe} gives an estimate of the intensity of the interaction between two Xe atoms and σ_{Xe-Xe} is the effective diameter of the Xe atoms. Note that under these conditions and at the densities and temperatures considered in this work Xe is a liquid.

The coupling between the I_2 vibration and the bath is described by the interaction Hamiltonian [see Eq. (2c)]. If vibration and translation were not coupled in the I_2, this term would just account for the interaction between the I_2 with the Xe atoms and, therefore, would look like Eq. (4), with ϵ_{Xe-Xe} and σ_{Xe-Xe} replaced by ϵ_{I_2-Xe} and σ_{I_2-Xe}, and r_{ij} replacing r_{0i} between the I_2 and the ith Xe atom. In such a case, ϵ_{I_2-Xe} and σ_{I_2-Xe} can be taken as the average of the corresponding Xe-Xe and I_2-I_2 interactions, i.e., $\epsilon = \sqrt{\epsilon_{Xe-Xe}\epsilon_{I_2-I_2}}$ and $\sigma_{I_2-Xe}^{(0)} = (\sigma_{Xe-Xe}+\sigma_{I_2-I_2})/2$ (here, $\epsilon_{I_2-I_2} = 382.27$ cm^{-1} and $\sigma_{I_2-I_2} = 4.982$ Å denote the well-depth and position of the minimum for the corresponding I_2-I_2 pairwise Lennard-Jones potential function). Here, however, since the diatomic is "breathing" while it vibrates, σ plays the role of an effective radius given by $\sigma_{I_2-Xe} = (\sigma_{Xe-Xe} + \sigma_{I_2-I_2} + \alpha q)/2 = \sigma_{I_2-Xe}^{(0)} + \alpha q/2$ [38]. Since diatoms expand and contract in one direction, $\alpha \lesssim 1$. This model, termed an effective breathing sphere, models the interaction of I_2 with the surrounding environment through the interaction potential:

$$\phi_{I_2-Xe}(r_{0i}, q) = 4\epsilon_{I_2-Xe}\left[\left(\frac{\sigma_{I_2-Xe}}{r_{0i}}\right)^{12} - \left(\frac{\sigma_{I_2-Xe}}{r_{0i}}\right)^6\right],$$
(5)

a potential that is known [38] to be quantitatively reliable for this system.

To obtain the analog of an uncoupled oscillator bath for comparison purposes, we simply ignore the Xe-Xe interactions, setting the third term in Eq. (2b) to zero. Collisional interactions between the Xe atoms of the bath are thus removed, although collisions with the I_2 are retained, a model referred to below as the "Xe ideal gas".

B. Dynamics

We consider initial states consisting of a thermally equilibrated Xe bath within which is embedded an iodine molecule in a superposition of vibrational states. Conceptually, such a superposition could be prepared by laser excitation from the ground vibrational state, where a multiphoton path can be utilized to overcome any selection rule issues. The subsequent dynamics calculations are done by sampling the Wigner distributions corresponding to the initial superpositions of Morse eigenstates [39] with classical trajectories [40], followed by standard Molecular Dynamics (MD) techniques [41] using the velocity-Verlet algorithm [42] to propagate the trajectories. The result is the time-evolving density $\rho(q, p, r_0, p_0, \{r_i, p_i\}_{i=1}^N, t)$ for the full system + bath. A total number of 2×10^6 trajectories was considered. In all reported simulations the total number of particles (I_2 plus Xe atoms) is 512, which was found to be adequate to converge the calculation of the purity, used as a measure of the system coherence. Finally, a density (I_2 in Xe) $\rho^* = 3053$ g/cm^3 was used in all the calculations to fix the size of the MD cell. Conversion factors and parameters used in the simulation are provided in the Appendix.

III. COMPUTATIONAL RESULTS AND DISCUSSION

As a measure of decoherence, we compute the purity χ of the I_2 dynamics [43], defined as

$$\chi = \text{Tr}[\rho_s^2(t)] = \int \rho_s^2(q, p, t)dqdp,$$
(6)

where

$$\rho_s(q, p, t) = \int \rho(q, p, r_0, p_0, \{r_i, p_i\}_{i=1}^N, t)dr_0 dp_0 \Pi_{i=1}^N dr_i dp_i$$
(7)

is the reduced density associated with the subsystem of interest, which here is the I_2 vibrational degree of freedom. Since the initial state (a vibrational superposition) is described by a wavefunction, the purity is initially unity, but decays with time as a consequence of the entanglement of the system and bath degrees of freedom. A small amount of decay in χ is also observed as a function of time for the isolated diatomic propagated in the absence of the bath. This decay [see, e.g., Fig. 1] is a measure of the computational accuracy and is found to be very small over the relevant 5 ps time scale.

Figure 1(a) shows the purity as a function of time for the two cases of Xe liquid and Xe ideal gas where the initial vibrational degree of freedom of the I_2 is in an equal superposition of the ground and second excited vibrational state. At 177.36 K both liquid Xe and ideal gas Xe are seen to cause decoherence of I_2 on a picosecond time-scale. In this case it is apparent that the liquid Xe
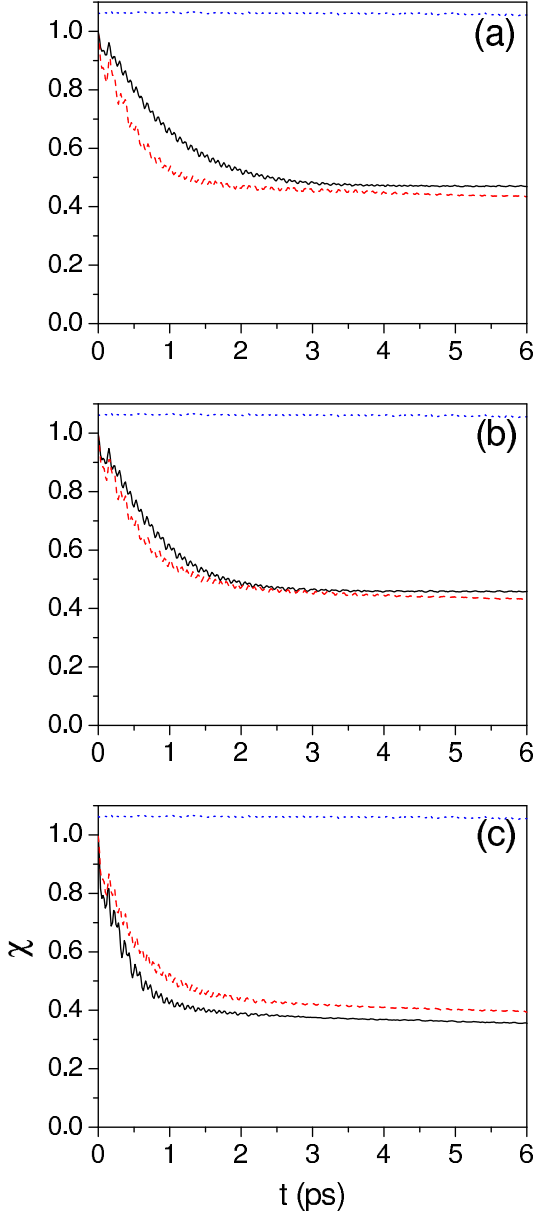
FIG. 1: Dependence on temperature of the purity as a function of time for the I_2 initially in a superposition of the ground and second-excited states: (a) $T = 177.36$ K, (b) $T = 221.7$ K and (c) $T = 554.25$ K. In all graphs, the black solid line indicates the Xe-Xe coupling is active, the red dashed line corresponds to the "ideal gas" bath (no intra-bath interactions), and the blue dotted line corresponds to the isolated I_2.
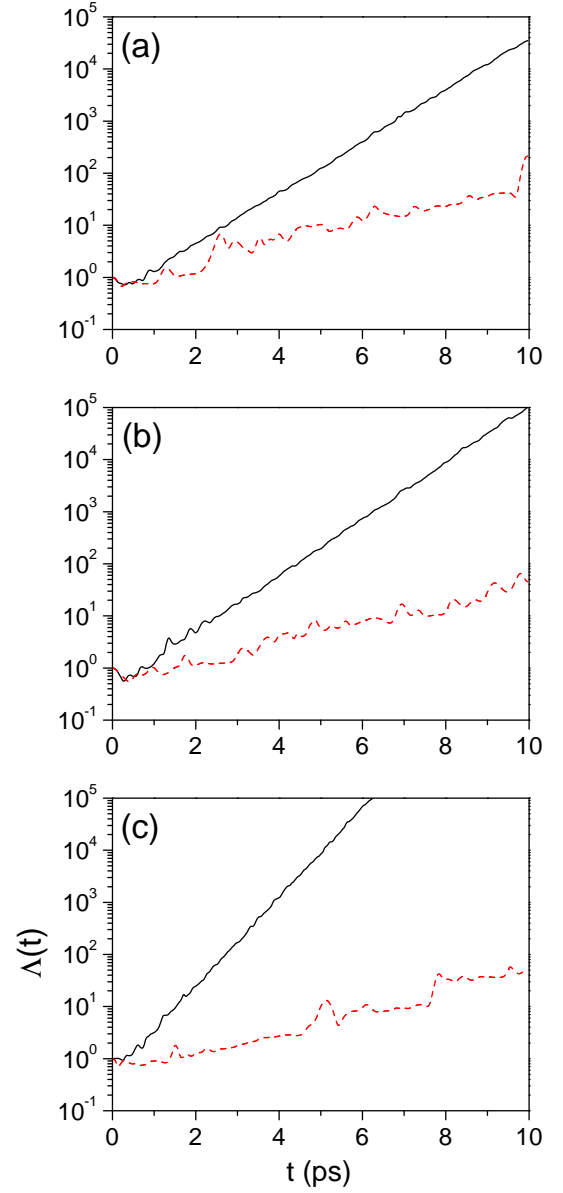
FIG. 2: Dependence on temperature of the Lyapunov exponent as a function of time for the I_2 initially in a superposition of the ground and second-excited states: (a) $T = 177.36$ K, (b) $T = 221.7$ K and (c) $T = 554.25$ K. In all graphs, the black solid line indicates the liquid Xe case and the red dashed line indicates the ideal gas Xe results. Note how $\Lambda(t)$ is similar in all three cases for the ideal gas Xe bath case.

bath causes substantially less decoherence than does the ideal gas Xe bath.

To verify that the liquid Xe dynamics is indeed chaotic we calculated the Lyapunov exponent, denoted by $\Lambda(t)$, as the distance between two nearby Xe initial conditions [44], which is known to grow exponentially for a chaotic distribution dynamics and sub-exponentially for integrable dynamics. Examination of the Lyapunov exponent $\Lambda(t)$ as a function of time for the two cases [see

Fig. 2(a)] clearly shows exponential growth for liquid Xe and sub-exponential growth for ideal gas Xe. Hence, the liquid Xe is chaotic, whereas the "ideal gas" case is not. The results shown in Figure 1 support the Alicki conjecture that bath chaos tends to suppress decoherence at low temperatures.

Similar results to those above are obtained at a temperature of 221.7 K. Figures 1(b) and 2(b) show the purity and Lyapunov exponents, respectively, plotted against time for the two cases for the same 0-2 superposition.

The liquid Xe shows the expected exponentially increasing dependence of $\Lambda(t)$ with time, showing that the bath is chaotic. Indeed, the slope of the logarithm of $\Lambda(t)$ has increased, suggesting that the liquid is even more chaotic than at the lower temperature. Again, the liquid Xe case is found to induce less decoherence than does the ideal gas Xe, but the difference between them is now less pronounced.

The situation at high temperature, however, is quite different. As seen in Fig. 1(c), at 554.25 K liquid Xe bath causes greater decoherence than does the ideal gas Xe. The Lyapunov exponent displayed in Fig. 2(c) confirms that liquid Xe bath is chaotic, with an even larger Lyapunov exponent [as manifest in the slope of $\Lambda(t)$ versus t]. Thus, a transition has occurred from a low temperature regime where the bath chaotic bath induces less decoherence than does the non-collisional bath, to a high temperature regime where the reverse is the case.

It is evident from Fig. 3 that the decoherence dynamics for the integrable "ideal gas" case is relatively unchanged as a function of temperature. Hence, it is the chaotic case that goes from weak to strong decoherence as the temperature increases, and is responsible for the cross-over behavior in the decoherence of regular versus chaotic baths.

To verify that this transition occurs for other initial conditions we also show simulations for a second coherent vibrational superposition state. Figures 3(a)-(c) show the purity as a function of time for three different temperatures (177.36, 221.7, and 554.25 K) calculated for a coherent superposition of the fifth and eighth vibrational states of the I_2. The decay of the purity is faster for this second initial state than it is for the first. Here the dynamics appears to occur on two time-scales, a fast initial decay followed by a slower falloff. The fast initial decay is common to both the liquid and ideal gas simulations. Otherwise the plots are qualitatively similar to those for the first initial state examined above. Significantly, the cross-over at high temperatures is again apparent: Decoherence of the liquid is smaller than that of the ideal gas at 177.36 and 221.7 K, but larger at the highest temperature 554.25 K.

IV. CONCLUSIONS

We have explicitly compared decoherence in the same system immersed in a liquid Xe bath, a well known paradigmatic system. In doing so we have confirmed that subsystems interacting with condensed phase environments cannot be analyzed using approaches that neglect intra-environmental coupling within the bath. Further, we demonstrated that this coupling leads to a cross-over in the decoherence dynamics as a function of temperature.

The transition described in the previous section has not been previously observed computationally. It is clear that the integrable bath case, in the liquid domain, is
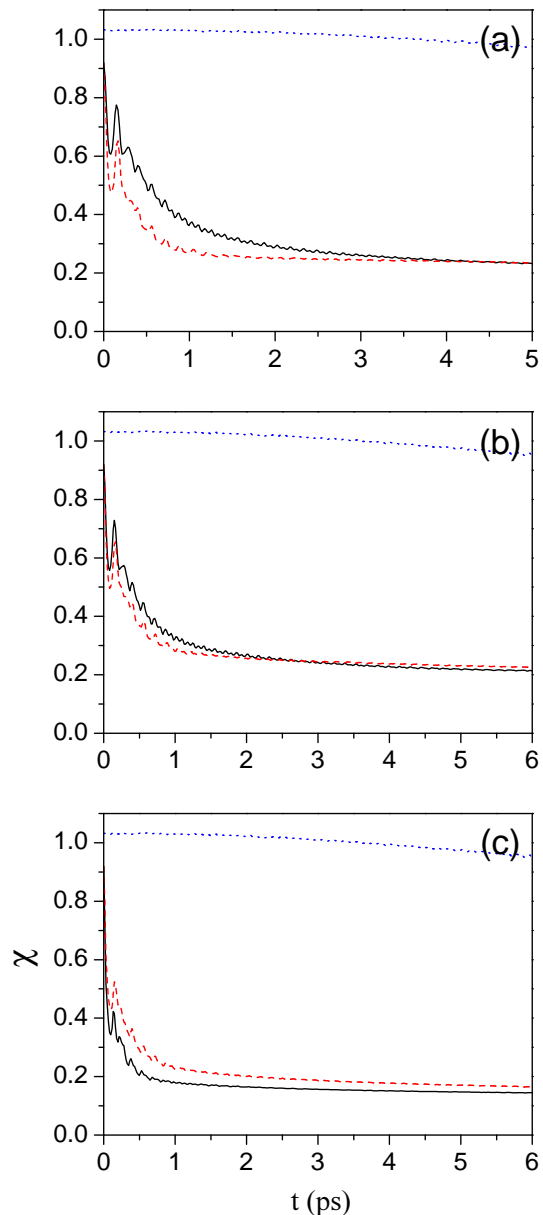

FIG. 3: Dependence on temperature of the purity as a function of time for the I_2 initially in a superposition of the fifth-and eighth-excited states: (a) $T = 177.36$ K, (b) $T = 221.7$ K and (c) $T = 554.25$ K. In all graphs, the black solid line indicates the Xe-Xe coupling is active, the red dashed line indicates the off coupling situation, and the blue dotted line indicates the isolated I_2.

relatively insensitive to temperature whereas the chaotic shows increasing decoherence with increasing temperature. Since the chaotic bath case displays weaker coherence than the integrable bath case at low temperature, the increasing decoherence of the chaotic case with temperature results in a cross-over of behavior. The low decoherence of the chaotic case at low temperatures is in accord with the analysis in terms of spectral properties of the bath. What is remarkable to note is that the Wigner

method is capable of properly displaying this behavior.

The results suggest a more detailed analysis of the origins of the difference between the chaotic and integrable baths in different density regions and the interrelationship between the rates of decoherence and the Lyapunov exponent of the chaotic bath would be of interest. Work on such systems is planned.

Computational aspects

The MD simulations were carried out using well-known standard procedures [41]. All the parameters involved were re-scaled taking into account the parameters associated with the solvent particles (here, the Xe atoms). That is:

interparticle distance: $r^* = r/\sigma_{Xe-Xe}$,
time: $t^* = \eta t$,
frequency: $\omega^* = \omega/\eta$,
density: $\rho^* = \sigma_{Xe-Xe}^3 \rho$,
temperature: $T^* = k_B T/\epsilon_{Xe-Xe}$,

with $\eta = \sqrt{\epsilon_{Xe-Xe}/m_{Xe}\sigma_{Xe-Xe}^2}^{1/2} \simeq 3.015 \times 10^{11}$ s^{-1} (i.e., 1 MD time unit is equivalent approximately to

3.32 ps) and where the magnitudes with asterisk denote the re-scaled magnitudes. Thus, for example, a density $\rho^* = 0.85$ will corresponds to $\rho = 3.053$ g/cm^3 and a temperature $T^* = 1.26$ to $T = 280$ K, while Planck's constant will become $\hbar^* = \hbar/\sqrt{m_{Xe-Xe}\sigma_{Xe-Xe}^2\epsilon_{Xe-Xe}} \simeq 0.010388$. This scaling leads to a system of dimensionless equations of motion, which are solved by means of the standard velocity-Verlet method in the case of both the system and the environment. Within this scheme, quantum features are taken into account initially in terms of the classical Wigner method, i.e., by carrying out a Monte Carlo sampling based on the Wigner distribution of the initial state of the I$_2$ vibrational state.

The constants of solute and solvent are those previously obtained for the Xe + I$_2$ system [38], i.e., $\epsilon_{I_2-I_2}/k_B = 550$ K, $\sigma_{I_2-I_2} = 4.982$ Å, $\epsilon_{Xe-Xe}/k_B = 221.7$ K and $\sigma_{Xe-Xe} = 3.930$ Å ($k_B = 1.3806505 \times 10^{-23}$ J/K being Boltzmann's constant). The solute and solvent masses are, respectively, $m_0 = 4.22 \times 10^{-22}$ g and $m_s = 2.18 \times 10^{-22}$ g. Now, taking into account the re-scaling, we will find $m_{Xe}^* = 1$, $\sigma_{Xe-Xe}^* = 1$ and $\epsilon_{Xe-Xe}^* = 1$ for the Xe atoms, while $m_{I_2}^* = 1.936$, $\sigma_{I_2}^* = 1.268$ and $\epsilon_{I_2}^* = 2.481$. Regarding the I$_2$ vibrational degree of freedom, we will find that $D^* = 81.4208$, $\beta^* = 7.30037$ and $\mu_{I_2}^* = 0.4839$. The vibrational frequency corresponding to the I$_2$ is $\omega_{I_2} = \sqrt{2\beta^2 D/\mu_{I_2}} = 4.0451 \times 10^{13}$ s^{-1}, which in MD reduced units becomes $\omega_{I_2}^* = 134.16$ in reduced MD units (the period, in these MD units, is therefore $\tau = 2\pi/\omega \simeq 0.0468$).

[1] M.A. Nielsen and I.L. Chuang, *Quantum Computation and Quantum Information* (Cambridge University Press, Cambridge, 2000).

[2] M. Shapiro and P. Brumer, *Principles of the Quantum Control of Molecular Processes* (Wiley-Interscience, Hoboken, 2003); *Quantum Control of Molecular Processes* (Wiley-VCH, Weinheim, 2011).

[3] W.H. Zurek, Nature (London) **412**, 712 (2001).

[4] S. Paganelli, F. de Pasquale, and S.M. Giampaolo, Phys. Rev. A **66**, 052317 (2002).

[5] R. Blume-Kohout and W.H. Zurek, Phys. Rev. A **68**, 032104 (2003).

[6] L. Tessieri and J. Wilkie, J. Phys. A **36**, 12305 (2003).

[7] R. Alicki, Open Syst. & Inf. Dyn. **11**, 53 (2004).

[8] M. Lucamarini, S. Paganelli, and S. Mancini, Phys. Rev. A **69**, 062308 (2004).

[9] C.M. Dawson, A.P. Hines, R.H. McKenzie, and G.J. Milburn, Phys. Rev. A **71**, 052321 (2005).

[10] X.S. Ma, A.M. Wang, X.D. Yang, and H. You, J. Phys. A **38**, 2761 (2005).

[11] X.-Z. Yuan and K.-D. Zhu, Europhys. Lett. **69**, 868 (2005).

[12] X.-Z. Yuan, K.-D. Zhu, and Z.-J. Wu, Eur. Phys. J. D **33**, 129 (2005).

[13] J. Lages, V.V. Dobrovitski, M.I. Katsnelson, H. A. De Raedt, and B.N. Harmon, Phys. Rev. E **72**, 026225 (2005).

[14] M. Çetinbaş and J. Wilkie, Phys. Lett. A **370**, 194 (2007).

[15] A.O. Caldeira and A.J. Leggett, Ann. Phys. **149**, 374 (1983).

[16] C. Anastopoulos and B.L. Hu, Phys. Rev. A **62**, 033821 (2000).

[17] R.P. Feynman and F.L. Vernon, Jr., Ann. Phys. **24**, 118 (1963).

[18] A.O. Caldeira and A.J. Leggett, Physica A **121**, 587

(1983).

[19] F. Haake and R. Reibold, Phys. Rev. A **32**, 2462 (1985).

[20] N.V. Prokof'ev and P.C.E. Stamp, Rep. Prog. Phys. **63**, 669 (2000).

[21] M.R. Gallis and G.N. Fleming, Phys. Rev. A **43**, 5778 (1991); L.E. Ballentine, Phys. Rev. A **43**, 9 (1991).

[22] M. Tegmark and L. Yeh, Physica A **202**, 342 (1994).

[23] J.A. Shields, M.E. Msall, M.S. Carroll, and J.P. Wolfe, Phys. Rev. B **47**, 12510 (1993).

[24] T. Miyano, S. Munetoh, K. Moriguchi, and A. Shintani, Phys. Rev. E **64**, 016202 (2001).

[25] E.R. Mucciolo, R.B. Capaz, B.L. Altshuler, and J.D. Joannopoulos, Phys. Rev. B **50**, 8245 (1994).

[26] P. Gaspard, M.E. Briggs, M.K. Francis, J.V. Sengers, R.W. Gammon, J.R. Dorfmann, and R.V. Calabrese, Nature (London) **394**, 865 (1998).

[27] S. Yuan, M.I. Katsnelson, and H. De Raedt, Phys. Rev. A **75**, 052109 (2007); Phys. Rev. B **77**, 184301 (2008).

[28] A. Relaño, J. Dukeslky, and R. A. Molina, Phys. Rev. E **76**, 046223 (2007).

[29] C.-Y. Lai, J.-T. Hung, C.-Y. Mou, and P. Chen, Phys. Rev. B **77**, 205419 (2008).

[30] W. Yang and R.-B. Liu, Phys. Rev. B **78**, 085315 (2008).

[31] L.-C. Nie Jing Wang, and X.-X. Yi, Commum. Theor. Phys. **51**, 815 (2009).

[32] A. Relaño, J. Stat. Mech., P07016 (2010).

[33] B. Erbe and J. Schliemann, Phys. Rev. Lett. **105**, 177602 (2010).

[34] J. Wilkie and P. Brumer, Phys. Rev. A **55**, 43 (1997); T. Prosen, Ann. Phys. **235**, 115 (1994); M. Feingold and A. Peres, Phys. Rev. A **34**, 591 (1986); P. Pechukas, Phys. Rev. Lett. **51**, 943 (1983).

[35] J. Wilkie (private communication); For related background see M. Çetinbaş and J. Wilkie, Phys. Lett. A **372**, 990 (2008); M. Çetinbaş and J. Wilkie, Phys. Lett. A **372**, 1194 (2008).

[36] J. Gong and P. Brumer, Phys. Rev. Lett. **90**, 050402 (2003); J. Mod. Opt. **50**, 2411 (2003).

[37] Y. Elran and P. Brumer, J. Chem. Phys. **121**, 2673 (2004).

[38] S.A. Egorov and J.L. Skinner, J. Chem. Phys. **105**, 7047 (1996).

[39] C. Mündel and W. Domcke, Chem. Phys. **105**, 137 (1986).

[40] Y. Elran and P. Brumer (unpublished).

[41] D. Frenkel and B. Smit, *Understanding Molecular Simulation*, 2nd ed. (Academic, New York, 2002).

[42] M.P. Allen and D.J. Tildesley, *Computer Simulation of Liquids* (Clarendon, Oxford, 1987).

[43] X.-P. Jiang and P. Brumer, Chem. Phys. Lett. **208**, 179 (1993).

[44] R. H. Miller, Astroph. J. **140**, 250 (1964); A.K. Pattanayak and P. Brumer, Phys. Rev. Lett. **77**, 59 (1996); Phys. Rev. E **56**, 5174 (1997); D. Gerbasi, A.S. Sanz, P.S. Christopher, M. Shapiro, and P. Brumer, J. Chem. Phys. **126**, 124307 (2007).